Supporting Information

Sellis et al. 10.1073/pnas.1114573108

SI Text

Definitions. In Fisher's geometric model (1–5), phenotypes are represented by vectors $\boldsymbol{r}$ that exist in a d-dimensional Euclidean phenotype-space $\mathbb{P} = \mathbb{R}^d$. In haploids, the genotype space $\mathbb{G}_{\text{hap}}$ is isomorphic to the phenotype space, and it is therefore convenient simply to label alleles by their corresponding phenotype $\boldsymbol{r}$ and work directly with phenotypes. Mutations are modeled by adding a mutation vector $\boldsymbol{m}$ to the mutated allele (i.e., $\boldsymbol{r} \to \boldsymbol{r} + \boldsymbol{m}$). We assume that mutational direction is sampled from a uniform distribution and that mutational magnitudes are sampled from a specified probability distribution $P(m)$.

The phenotype of a diploid organism $\boldsymbol{r}_{xy}$ is the product of two constituent alleles $\boldsymbol{r}_x$ and $\boldsymbol{r}_y$; thus, to incorporate diploidy, we must define the mapping from the diploid genotype to the organismal phenotype. The organismal phenotype space for diploids is identical to that for haploids, $\mathbb{P} = \mathbb{R}^d$, whereas the diploid genotype space is the direct product of two allelic genotype spaces, each of which is isomorphic to the organismal phenotype space (i.e., $\mathbb{G}_{\text{dip}} = \mathbb{R}^d \otimes \mathbb{R}^d$). We are free to label individual alleles by the organismal phenotype they produce when homozygous (i.e., $\boldsymbol{r}_i = \boldsymbol{r}_{ii}$). We then define the diploid genotype-phenotype mapping as the weighted average of the two constituent alleles: $\boldsymbol{r}_{xy} = (c_x\boldsymbol{r}_x + c_y\boldsymbol{r}_y)/(c_x + c_y)$. The weighting represents the phenotypic dominance relationship between the alleles. Because of the direct relation between allelic genotypes and organismal phenotypes in diploids, it is again convenient to elide the genotype-phenotype map and speak simply of allelic "phenotypes" analogous to haploid phenotypes, which mutate analogously to those haploid phenotypes as well.

In our theoretical analysis, we focus on the specific situation of a mutant allele $\boldsymbol{r}_a + \boldsymbol{m}$ arising in a population initially monomorphic for the wild-type allele $\boldsymbol{r}_a$. It is then convenient to express the phenotype of the mutant heterozygote as $\boldsymbol{r}_{ab} = \boldsymbol{r}_a + h\boldsymbol{m}$, where h specifies the phenotypic dominance relation of the mutation $\boldsymbol{m}$ with respect to the wild type.

To map organismal phenotype to fitness, we define a fitness function $w(\boldsymbol{r})$. We restrict our consideration to fitness functions that depend only on the distance from an optimal phenotype and are monotonically decreasing in distance from that optimum. For convenience, we set the origin to be at the fitness optimum; hence, $w(\boldsymbol{r}) \to w(r)$.

Range of Adaptive Mutant Alleles. Adaptive mutations are those that increase the fitness of organisms carrying the mutant allele $\boldsymbol{r}_b = \boldsymbol{r}_a + \boldsymbol{m}$. Given our assumptions about the form of the fitness function, this requires that $|\boldsymbol{r}_b| < r_a$ in haploids. In diploids, under the Hardy–Weinberg assumptions, it is the fitness of the mutant heterozygote that primarily determines the probability of a new mutation invading the population. This makes it convenient to define adaptive mutations in diploids as those that are adaptive immediately on origination as a heterozygote (i.e., $|\boldsymbol{r}_{ab}| < r_a$). Thus, the range of adaptive mutant alleles in haploids (α_{hap}) and diploids (α_{dip}) is described by:

$$\alpha_{\text{hap}} = \{\boldsymbol{r}_b : |\boldsymbol{r}_b| < r_a\} \qquad \text{[S1]}$$

$$\alpha_{\text{dip}} = \left\{\boldsymbol{r}_b : \left|\boldsymbol{r}_b - \frac{-(1-h)}{h}\boldsymbol{r}_a\right| < \frac{r_a}{|h|}\right\}. \qquad \text{[S2]}$$

Both are spheres: α_{hap} has radius r_a and is centered at the origin, and α_{dip} has radius $r_a/|h|$ and is centered at $-((1-h)/h)\boldsymbol{r}_a$.

In diploids, we also wish to distinguish between those adaptive mutations that are expected to replace the wild type [i.e., $w(\boldsymbol{r}_{bb}) > w(\boldsymbol{r}_{ab}) > w(\boldsymbol{r}_{aa})$] and those that are not expected to do so because they have heterozygote advantage [i.e., $w(\boldsymbol{r}_{bb}) < w(\boldsymbol{r}_{ab}) > w(\boldsymbol{r}_{aa})$]. The range of replacing mutant alleles (γ) is given by:

$$\gamma = \begin{cases} \emptyset & h < 0 \\ r_b : \left|r_b - \dfrac{h}{1+h}\boldsymbol{r}_a\right| < \dfrac{r_a}{1+h} & 0 < h < 1 \\ r_b : \left|r_b - \dfrac{h}{1+h}\boldsymbol{r}_a\right| > \dfrac{r_a}{1+h} & h > 1. \end{cases} \qquad \text{[S3]}$$

For incomplete phenotypic dominance ($0 < h < 1$), γ is a sphere of radius $r_a/(1 + h)$ centered at $h/(1 + h)\boldsymbol{r}_a$. For phenotypic overdominance ($h > 1$), the direction of the inequality is switched and γ is all points that are excluded from this sphere (but that fall in α_{dip}). The range of adaptive mutants that have heterozygote advantage is then α_{dip} without γ. Note that α_{hap}, α_{dip}, and γ are collinear spheres and $\boldsymbol{r}_a$ lies on the surface of each (Fig. 2*A*).

Probability of Adaptive Mutations. The probability that a mutation in this model is adaptive can be expressed as a purely geometric question: What is the probability that the end point of a vector originating on the surface of a sphere (the mutation) will lie within that sphere (the range of adaptive mutants), given that the vector's direction is sampled uniformly? This probability, $P < (m/R;d)$, depends on the ratio of the magnitude of the vector $\boldsymbol{m}$ to the radius of the sphere R and the dimensionality d. For convenience, let the origin of our space be at the center of the sphere. We choose $\boldsymbol{R}$ to be the point on the sphere's surface from which the vector originates. The condition for the end point to lie within the sphere is:

$$|\boldsymbol{R} + \boldsymbol{m}| < R \Leftrightarrow \cos(\phi) > \frac{m}{2R}. \qquad \text{[S4]}$$

Here, ϕ is π minus the angle between $\boldsymbol{m}$ and $\boldsymbol{R}$. Note that this inequality can only be satisfied if m is less than $2R$, because $\cos(x) \le 1$. We can determine $P < (m/R;d)$ by enforcing the condition on ϕ, while integrating over all orientations of $\boldsymbol{m}$:

$$p < (m/R;d) = \frac{\int_0^{\cos^{-1}\left(\frac{m}{2R}\right)} \left[\frac{m}{2R}\sin(\phi)\right]^{d-2} \mathrm{d}\phi}{\int_0^{\pi} \left[\frac{m}{2R}\sin(\phi)\right]^{d-2} \mathrm{d}\phi}, \qquad \text{[S5]}$$

$$= \frac{1}{2} - \frac{m}{2R}\frac{\Gamma\left(\frac{d}{2}\right)}{\sqrt{\pi}\Gamma\left(\frac{d+1}{2}\right)}{}_2F_1\left[\frac{1}{2}, \frac{3-d}{2}, \frac{3}{2}, \left(\frac{m}{2R}\right)^2\right]. \qquad \text{[S6]}$$

The probability function $P < (m/R;d)$ is monotonically decreasing over the relevant range of $0 < m \le 2R$ for all dimensionalities. Two special values deserve mention: $P < (0, d) = 1/2$ and $P < (2, d) = 0$ independent of dimension. The shape of $p < (m/R;d)$ for several dimensionalities is shown in Fig. S7. We compare this exact result with a long-standing approximation used in the study of Fisher's geometric model (1–3), that $p < (m/R, d) \approx \int_{\frac{m}{2R}\sqrt{d}}^{\infty} e^{-\frac{t^2}{2}}\mathrm{d}t$. This approximation is very good at high dimensions, which pre-

vious studies assumed, but deviates significantly at low dimensions (Fig. S7). This can be important when exploring Fisher's geometric model at these lower dimensionalities, as in our simulations performed at $d = 2$.

Adaptive Mutations in Haploids and Diploids. Let α be the range of adaptive mutations, and assume that the mutation supply is identical for haploids and diploids. The rate at which adaptive mutations occur in a monomorphic population (u) is then:

$$u = \frac{\Theta}{2}\int_{\alpha} P(\boldsymbol{m})\mathrm{d}\boldsymbol{m} = \frac{\Theta}{2}\int_{0}^{\infty} P(m)p_<(m/R_\alpha;d)\mathrm{d}m. \qquad [S7]$$

Here, $\Theta/2 = cN\mu$ (c, ploidy level; N, population size; μ, mutation rate per individual) is the overall rate at which mutations occur in the population. We have used the fact that α is a sphere with the wild-type allele on its boundary in this model. R_α is the radius of the adaptive region; $R_\alpha = \boldsymbol{r}_a$ for haploids and $R_\alpha = r_a/|h|$ for diploids.

We further define the rate at which adaptive mutations invade the population (υ) and the average initial selective effect of adaptive mutations (Δw):

$$\upsilon = \frac{\Theta}{2}\int_{\alpha} P(m)\pi(\boldsymbol{m})\mathrm{d}\boldsymbol{m}, \qquad [S8]$$

$$\langle \Delta w \rangle = \frac{\Theta}{2\upsilon}\int_{\alpha} P(m)\pi(\boldsymbol{m})\Delta w(\boldsymbol{m})\mathrm{d}\boldsymbol{m}. \qquad [S9]$$

The invasion probability $\pi(\boldsymbol{m})$ is proportional to $\Delta w(\boldsymbol{m})$, the fitness difference between the mutant individual and the wild-type fitness (2). In diploids, the mutant individual is heterozygous in the mutant allele, so $\pi_{\mathrm{dip}}(\boldsymbol{m}) \propto \Delta w_{\mathrm{dip}}(\boldsymbol{m}) = w(\boldsymbol{r}_a + h\boldsymbol{m}) - w(\boldsymbol{r}_a)$, whereas in haploids, $\pi_{\mathrm{hap}}(\boldsymbol{m}) \propto \Delta w_{\mathrm{hap}}(\boldsymbol{m}) = w(\boldsymbol{r}_a + \boldsymbol{m}) - w(\boldsymbol{r}_a)$.

We are particularly interested in the relative rates of adaptation in haploids and diploids. For that reason, we consider the ratios of u, υ, and $\langle w \rangle$ between haploids and diploids. We calculated these ratios numerically for different values of h and over a range of the parameter $\langle m \rangle$ using the exponential (Fig. S1) and uniform (Fig. S2) distributions of mutation sizes. Here, we focus on two limiting cases: (i) the "large-mutation" limit, where $P(m)$ is uniform over the entire range of adaptive mutations (which is the case in both the uniform mutation model and the exponential mutation model if $\langle m \rangle \gg r_a$), and ($ii$) the "small-mutation" limit, where $P(m)$ is nonzero only for infinitesimal mutations.

Large-Mutation Limit. In the large-mutation limit, $P(m)$ is constant over the entire range of adaptive mutations. The ratio of the rates of occurrence of new mutations $u_{\mathrm{dip}}/u_{\mathrm{hap}}$ is then:

$$\frac{u_{\mathrm{dip}}}{u_{\mathrm{hap}}} = \frac{\int_0^\infty P(m)p_<(|h|m/r_a;d)\mathrm{d}m}{\int_0^\infty P(m)p_<(m/r_a;d)\mathrm{d}m} = \frac{1}{|h|}. \qquad [S10]$$

This result is achieved by a change of variables $m' = |h|m$ in the numerator. Note that this result is the ratio of the radii of the respective adaptive ranges and is independent of dimension. For the ratio of the invasion rates υ, we have:

$$\frac{\upsilon_{\mathrm{dip}}}{\upsilon_{\mathrm{hap}}} = \frac{\int_{\alpha_{\mathrm{dip}}} P(m)\pi_{\mathrm{dip}}(\boldsymbol{m})\mathrm{d}\boldsymbol{m}}{\int_{\alpha_{\mathrm{hap}}} P(m)\pi_{\mathrm{hap}}(\boldsymbol{m})\mathrm{d}\boldsymbol{m}} = \frac{1}{|h|}. \qquad [S11]$$

Once again, this result is obtained by a change of variables, $\boldsymbol{m}' = |h|\boldsymbol{m}$. We made use of the fact that $h\alpha_{\mathrm{dip}} \equiv \alpha_{\mathrm{hap}}$ (i.e., "multiplying" a sphere by a constant results in another sphere). Finally, the ratio of the average initial selective increments $\langle \Delta w \rangle$ is as follows:

$$\frac{\langle \Delta w \rangle_{\mathrm{dip}}}{\langle \Delta w \rangle_{\mathrm{hap}}} = \frac{\upsilon_{\mathrm{hap}}}{\upsilon_{\mathrm{dip}}}\frac{\int_{\alpha_{\mathrm{dip}}} P(m)\pi_{\mathrm{dip}}(\boldsymbol{m})\Delta w_{\mathrm{dip}}(\boldsymbol{m})\mathrm{d}\boldsymbol{m}}{\int_{\alpha_{\mathrm{hap}}} P(m)\pi_{\mathrm{hap}}(\boldsymbol{m})\Delta w_{\mathrm{hap}}(\boldsymbol{m})\mathrm{d}\boldsymbol{m}} = 1. \qquad [S12]$$

Applicability of the Large-Mutation Limit. The large-mutation limit, as we have defined it, requires that the entire range of adaptations be accessible to mutation. In diploids, this means that mutations must reach a size of $2r_a/|h|$. However, our qualitative conclusions, such as the higher rate at which adaptive mutations arise in diploids under incomplete phenotypic dominance [$(0 < h < 1)$], will apply as long as the mutation supply reaches most of the range of adaptive mutations (i.e., $\langle m \rangle \sim r_a$). This condition can be relaxed even further at high dimension. In Fig. S7, we see that as dimensionality increases the range over which there are an appreciable number of adaptive mutations contracts (i.e., as dimension goes up), the characteristic size of potential adaptive mutations goes down. We can use the approximation $p_<(m/R,d) \approx \int_{\frac{m}{2R}\sqrt{d}}^{\infty} e^{-\frac{t^2}{2}}\mathrm{d}t$ to get a heuristic understanding of how this affects the applicability of the large-mutation limit. In this high-dimension approximation, m enters only in the combination $m\sqrt{d}/R$; R is effectively modified by $1/\sqrt{d}$. Therefore, the mutational supply reaches most adaptive mutations if:

$$\langle m \rangle \gtrsim \frac{r_a}{\sqrt{d}}. \qquad [S13]$$

The higher the dimensionality, the weaker is the condition on $\langle m \rangle$ and the more applicable the large-mutation limit becomes.

Small-Mutation Limit. In the small-mutation limit, all mutations are infinitesimal, as enforced by $P(m)$. Therefore, $P_<(m/R_\alpha;d) \sim P(0;d) = 1/2$. Clearly then, $u_{\mathrm{dip}} = u_{\mathrm{hap}}$ in this limit. Also, because the mutations are infinitesimal, a linear approximation to Δw is appropriate and $\Delta w_{\mathrm{dip}}(\boldsymbol{m}) = w(\boldsymbol{r}_a + h\boldsymbol{m}) - w(\boldsymbol{r}_a) \sim h\Delta w_{\mathrm{hap}}(\boldsymbol{m})$. So, $\upsilon_{\mathrm{dip}} \sim |h|\upsilon_{\mathrm{hap}}$ and $\langle \Delta w \rangle_{\mathrm{dip}} \sim |h|\Delta w_{\mathrm{hap}}$.

Heterozygote Advantage in Diploids. We now characterize the fraction of adaptive mutations in diploids that display heterozygote advantage (δ). We differentiate between δ_u, the fraction among all adaptive mutations, and δ_υ, the fraction among those that invade:

$$\delta_u = 1 - \frac{\int_\gamma P(m)\mathrm{d}\boldsymbol{m}}{\int_{\alpha_{\mathrm{dip}}} P(m)\mathrm{d}\boldsymbol{m}} \text{ and } \delta_\upsilon = 1 - \frac{\int_\gamma P(m)\pi_{\mathrm{dip}}(\boldsymbol{m})\mathrm{d}\boldsymbol{m}}{\int_{\alpha_{\mathrm{dip}}} P(m)\pi_{\mathrm{dip}}(\boldsymbol{m})\mathrm{d}\boldsymbol{m}}. \qquad [S14]$$

The small-mutation limit is trivial, α_{dip} and γ completely overlap for infinitesimal mutations, and homozygote mutants will never have lower fitness than heterozygotes for $0 < h < 1$, whereas all adaptive mutations will have heterozygote advantage if $h > 1$. Recall also that all adaptive mutations have heterozygote advantage when $h < 0$. The large-mutation limit derives immediately from our previous results concerning the ratios of rates between diploids and haploids. The only difference is that we are comparing α_{dip} with γ, which has a radius of $r_a/(1 + h)$. So, in the large-mutation limit:

$$\delta_u = \begin{cases} 1 & h < 0 \\ 1 - \dfrac{r_a/(1+h)}{r_a/h} = \dfrac{1}{1+h} & 0 < h < 1 \\ \dfrac{r_a/(1+h)}{r_a/h} = \dfrac{1}{1+h} & h > 1. \end{cases} \qquad [S15]$$

There are also two special cases: perfect phenotypic recessiveness $h = 0$ and perfect phenotypic dominance $h = 1$. In the case $h = 0$, mutations cannot be adaptive by our definition because their fitness as a heterozygote is not better than that of the wild type. In the case $h = 1$, the fitness of the mutant heterozygote is equal

to that of the mutant homozygote; thus, strictly speaking, there is never heterozygote advantage. We also note that in the special case of phenotypic codominance ($h = 1/2$), $\delta_u = 2/3$. Additionally, $\delta_u > 1/2$ for all values of h (except $h = 0,1$).

δ_v cannot be obtained by our previous methods; in this case, the π_{dip} terms in the numerator and denominator differ after the usual change of variables. In the case of $h = 1/2$, we made numerical calculations of δ_u and δ_v as a function of $\langle m \rangle$ for exponential and uniform distributions of mutation length, as shown in Figs. S1 and S2. Conditioning on invasion is always seen to increase the frequency of heterozygote advantage in the large-mutation limit.

Effectiveness of Heterozygote Advantage in the Presence of Drift. Selection is only consequential when it is strong enough to outcompete the stochastic fluctuations that arise from random genetic drift. In the context of balancing selection, this requires that the fitness advantage of the heterozygote over each homozygote has to be stronger than drift for balanced states to be effectively maintained.

Formally, the condition for selection to outcompete drift is that fitness differences have to be at least of order $1/N$ – the inverse of the population size (2). In our scenario of a symmetrical Gaussian fitness function, $w(r) = \exp[-r^2/(2\sigma_w^2)]$, this defines a sphere around the optimum of radius:

$$r_0 = \sqrt{-2\sigma_w^2 \log\left(1 - \frac{1}{N}\right)} \approx \sigma_w \sqrt{\frac{2}{N}}, \qquad \textbf{[S16]}$$

inside of which fitness will become effectively indiscernible from the optimal fitness. Once the population is located within this effectively neutral sphere, adaptation will cease. Similarly, if both the heterozygote and homozygote of a mutation with $w_{aa} < w_{ab} > w_{bb}$ (i.e., an adaptive mutation with heterozygote advantage) are located inside the sphere, selection will not be sufficient to stabilize the balanced state. The radius r_0 is proportional to the SD of the fitness function and decreases with the inverse square root of the population size.

The radius of the effectively neutral sphere sets a limit on how closely adaptive walks will approach the optimum. It also imposes a condition on the possibility of adaptation-driven balanced polymorphisms. It is required that $\langle m \rangle > r_0$ for the selection to be able to outcompete drift and maintain a balanced polymorphism. Heuristically, this can be understood as the requirement that mutations be able to span the neutral sphere, thereby allowing selection to distinguish between the homozygotes outside the sphere and the heterozygote within it. Note that this condition is different in kind from our previous condition for heterozygote advantage to be common, $\langle m \rangle \gtrsim r/\sqrt{d_a}$. Because r_a decreases over the course of an adaptive walk, we expect that although heterozygote advantage might not initially be frequent, it will eventually become so. The drift condition, however, does not change over the course of a walk; if it is not met, we expect drift to preclude the possibility of adaptation-driven balanced polymorphisms entirely.

Our heuristic explanation of the drift condition is appropriate at small dimensions; however, the consideration of large dimensions requires more care. In high-dimensional phenotypic spaces, most adaptive mutations are not primarily directed toward the optimum but, instead, are largely lateral displacements with just a small component in the direction of the optimum. Heterozygote advantage arises when the intermediate heterozygote is closer to the optimum than either homozygote (just as the midpoint of a chord is closer to the center of the circle than either end point). We can evaluate the possibility of heterozygote advantage in this situation, at least in the limit that $m << r_a$ (note that this is not inconsistent with our condition for frequent heterozygote advantage $\langle m \rangle \gtrsim r_a/\sqrt{d}$ when d is large). In this limit, the maximum decrease in the distance to the phenotypic optimum when comparing the mutant heterozygote with the fittest of the two homozygotes is approximately $\delta r = (m/2)^2/(2r)$. The selective advantage of the heterozygote can then be approximated as $w'(r)/w(r)\delta r$. Therefore, for the heterozygote advantage to exceed drift, given our Gaussian fitness function, it is necessary that $\langle m \rangle > \sigma_w \sqrt{2/N} = r_0$. Conveniently, this results in the same condition that we found previously (when we assumed that $m \approx r_a$). Thus, this serves as a universal condition for the possibility of adaptation-driven balanced polymorphisms in our model when accounting for drift. It should be noted that the identity between these low- and high-dimension conditions is a peculiarity of our choice of a Gaussian fitness function rather than a general feature of all single-peaked landscapes.

To verify these theoretical predictions, we simulated adaptive walks toward a fixed fitness optimum for various settings of N and σ_w, and $\langle m \rangle$. As previously, a 2D codominant Fisher's model was used, starting from a monomorphic population at $\boldsymbol{r}_a = (2,0)$; mutations were modeled by an exponential mutation-size distribution. We kept $\Theta = 0.1$ constant over all scenarios. Adaptive walks were simulated until either the population successfully adapted [as defined by at least 90% of individuals being located inside the effectively neutral sphere (i.e., $r_{ij} < r_0$)] or after $10N$ generations, whichever came first.

The results of these simulations are shown in Table S1 and summarized in Fig. 2*D*. As predicted by our theoretical arguments, consequential balanced states (e.g., where the fitness differences between heterozygotes and homozygotes are at least of size $1/N$) (as described in the section on ascertainment of balanced polymorphisms during adaptive walks in *Materials and Methods*) are always common in adaptive walks unless average mutation sizes $\langle m \rangle$ become on the order of r_0 or smaller. Interestingly, in our simulations, the presence of consequential balanced polymorphisms corresponds well with whether successful adaptation, as defined by the population traversing at least 90% of the initial fitness distance to the optimum, is observed at all. This results from the fact that when $m \approx r_a$ in our scenario, it is typical that $r_a \approx r_0$ also. Thus, in these cases, adaptive walks start already very close to the effectively neutral sphere; consequently, further fitness improvements can no longer outcompete the stochastic fluctuations attributable to drift.

1. Fisher RA (1930) *The Genetical Theory of Natural Selection* (Clarendon, Oxford).
2. Kimura M (1983) *The Neutral Theory of Molecular Evolution* (Cambridge Univ Press, Cambridge, UK).
3. Orr HA (1998) The population genetics of adaptation: The distribution of factors fixed during adaptive evolution. *Evolution* 52:935–949.
4. Hartl D, Taubes C (1998) Towards a theory of evolutionary adaptation. *Genetica* 102–103:525–533.
5. Orr HA (2005) The genetic theory of adaptation: A brief history. *Nat Rev Genet* 6(2): 119–127.

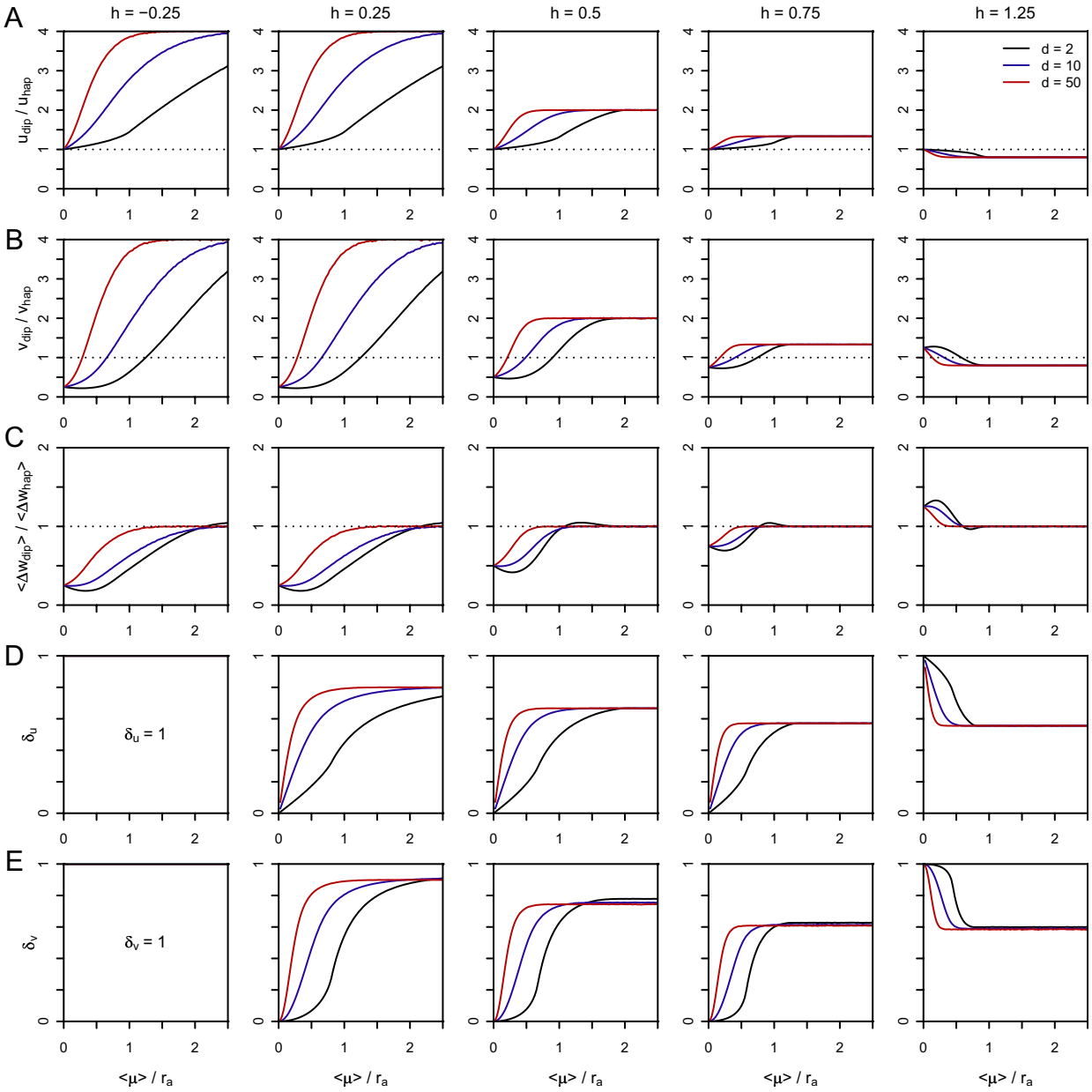

Fig. S1. Characteristics of single adaptive mutations in the uniform mutation model as a function of $\langle m \rangle / r_a$. The five columns span the range from phenotypic underdominance ($h = -0.25$) to overdominance ($h = 1.25$). Different colors show results for $d = 2$ (black), $d = 10$ (blue), and $d = 50$ (red) phenotypic dimensions. (*A*) Ratio of the rates at which new adaptive mutations occur. (*B*) Ratio of the rates of invading mutations. (*C*) Ratio of the average fitness advantage conferred by invading mutations. (*D*) Fraction of adaptive mutations in diploids that have heterozygote advantage. (*E*) Fraction of invading mutations in diploids that have heterozygote advantage.

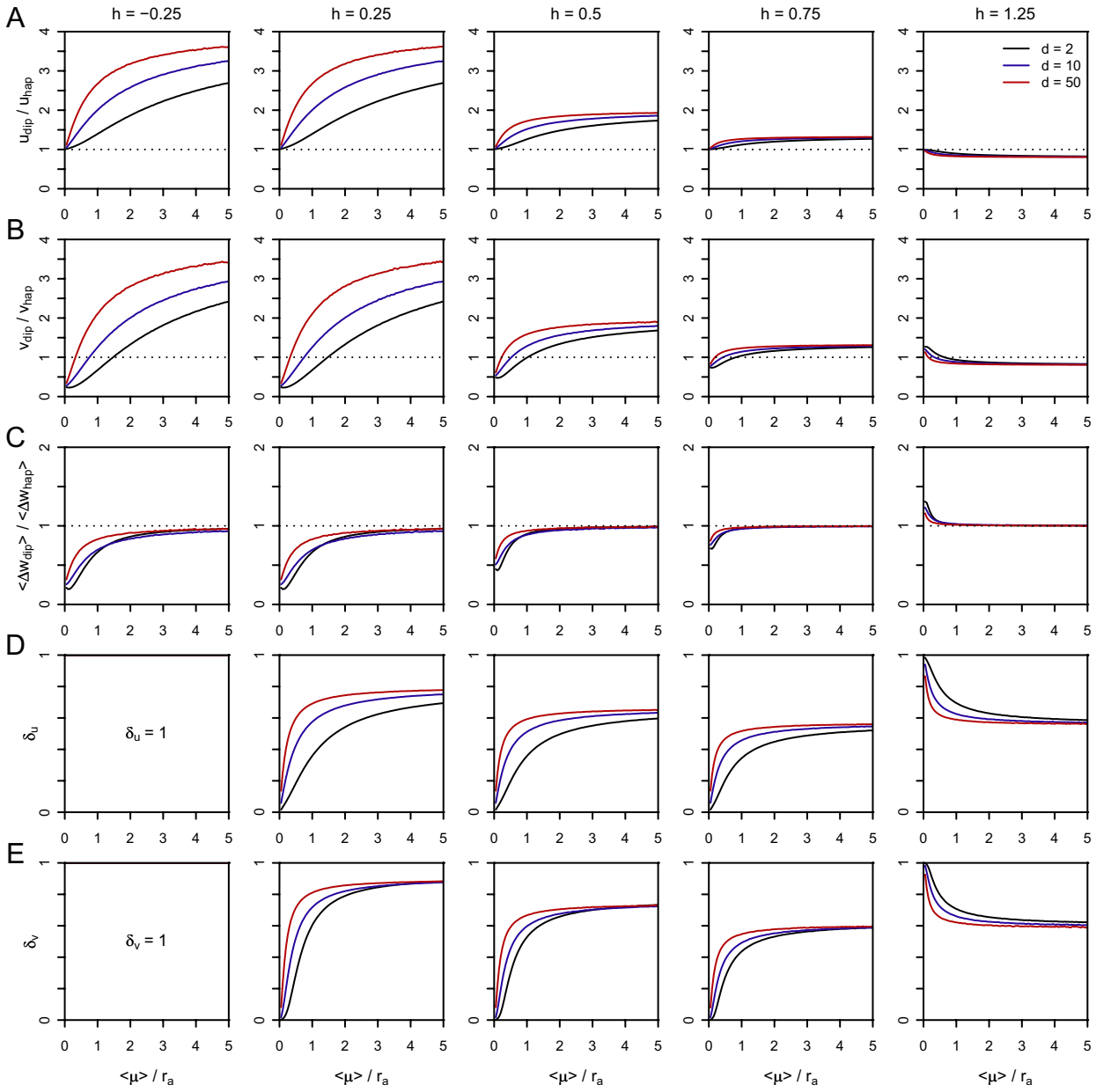

Fig. S2. Same as in Fig. S1, but data are shown for the exponential mutation model.

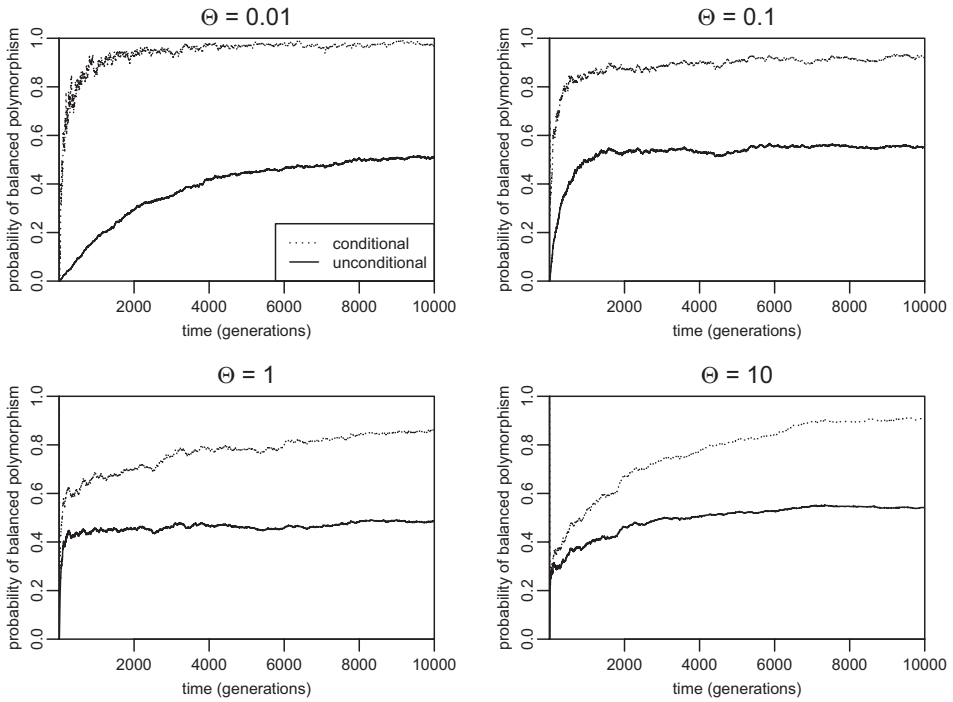

Fig. S3. Probability of observing a balanced polymorphism (frequency $0.05 < x < 0.95$) in a diploid population during adaptive walks toward a fixed optimum for different values of Θ. Solid lines are the absolute probabilities of observing a balanced polymorphism, and dotted lines are the probabilities conditional on the presence of a polymorphism. The mutation rate was always $\mu = 2.5 \times 10^{-7}$. Different values of $\Theta = 4N\mu$ correspond to different population sizes. Statistics were obtained by averaging over 10^2 walks for each value of Θ.

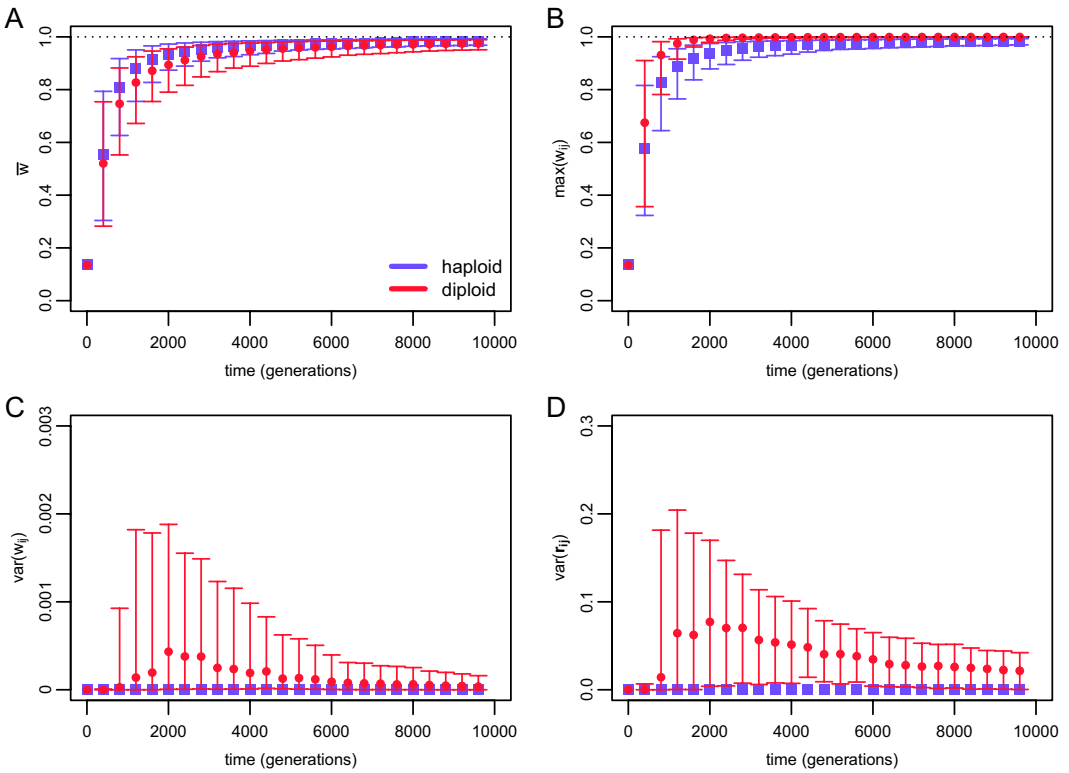

Fig. S4. Statistics of adaptive walks toward a fixed fitness optimum in haploid and diploid populations. (*A*) Mean population fitness ($\overline{w}$) in haploids is greater than that of the diploid population at all times when averaged over replicate walks. (*B*) Fitness of the most fit individual (w_{max}) is higher in diploids than it is in haploids at all time points when averaged over replicate walks. (*C*) Fitness variance over all individuals. Diploid populations suffer from a high genetic load, which can be identified as the segregation load attributable to pervasive fitness overdominance. (*D*) Genotypic variance over all individuals (calculated separately for each dimension and then summed over all dimensions). Data points are medians over 10^3 runs, and error bars specify the first and third quartiles.

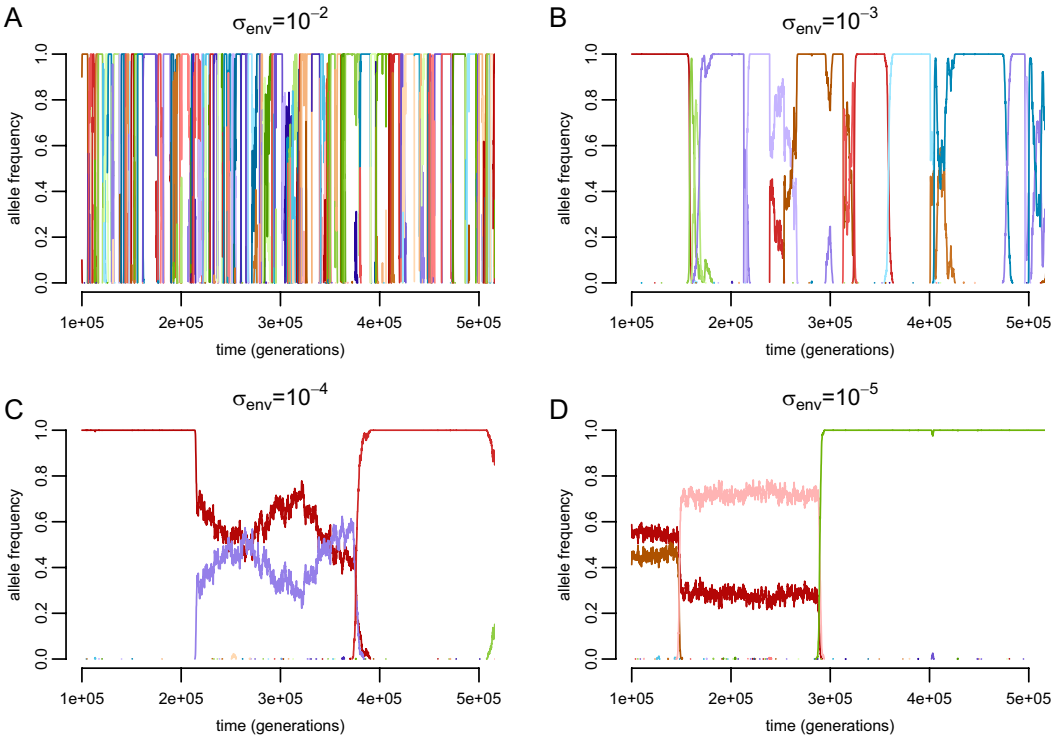

Fig. S5. Typical allele frequency trajectories in the moving optimum scenario. The four graphs show the trajectories of all alleles present during the first 5×10^5 generations of four simulation runs with different speeds of environmental change σ_{env}. Simulation parameters were $N = 5 \times 10^4$, $r_{aa} = (2,0)$, and $\langle m \rangle = \sigma_w = 1$ (*Materials and Methods*). Different colors represent different alleles. Under a fast-moving optimum (*A*), polymorphisms are shorter lived and adaptive alleles fix at a higher rate compared with a slow-moving optimum (*D*). The trajectories of balanced alleles in the moving optimum scenario differ from those in a fixed optimum scenario (Fig. 2*B*) in the frequency at which two alleles' balance may shift in response to the movement of the optimum, as can be seen in *B* and even more clearly in *C*.

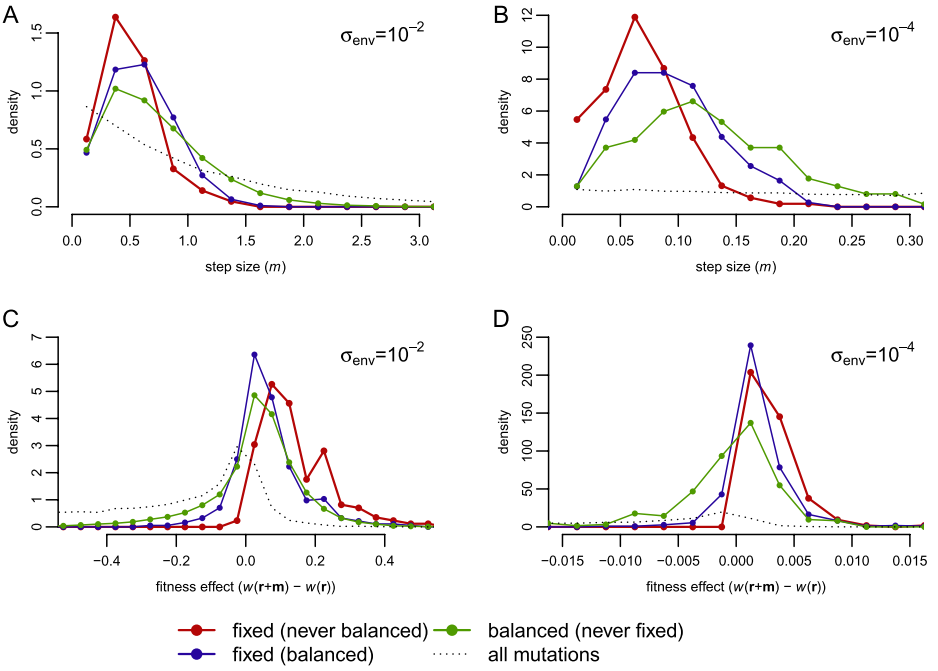

Fig. S6. Statistics of mutation effects in the moving optimum model. The two upper plots show the distributions of mutation sizes under a fast-moving optimum (*A*) and a slow-moving optimum (*B*) for different categories of mutations. Dotted lines indicate all newly occurring mutations specified by our standard exponential mutational model with $P(m) \propto \exp(-m)$, red indicates mutations that eventually became fixed in the population but were never part of a balanced polymorphism, blue indicates mutations that eventually became fixed but had previously been part of a balanced polymorphism, and green indicates mutations that were part of a balanced polymorphism but never became fixed. Average mutation sizes decrease, in order, from newly occurring mutations, balanced but never fixed mutations, balanced and eventually fixed mutations, to fixed but never balanced mutations. The fast- and slow-moving optimum scenarios show qualitatively similar behavior, with distributions being shifted toward larger sizes in the faster changing environment. The two lower plots show the distributions of fitness effects (mutant homozygote vs. wild-type homozygote) of the different mutation categories under fast-changing (*C*) and slow-changing (*D*) environments. Most newly occurring mutations in our model are deleterious as homozygotes. The fixed but never balanced mutations, as expected, confer the highest average homozygote fitness advantage. The fixed mutations that were intermediately balanced confer slightly lower average fitness advantage. Note that a substantial amount of these mutations initially have a negative fitness effect as homozygotes, as indicated by the below-zero tail of the distributions. Finally, the balanced mutations that never became fixed have the lowest fitness advantage as homozygotes. The fast- and slow-moving optimum scenarios again show qualitatively similar behavior, with distributions being shifted toward larger fitness differences in the faster changing environment. The distributions of mutation sizes and fitness effects in each scenario were estimated from 10^4 simulation runs over 10^7 generations each (*Materials and Methods*).

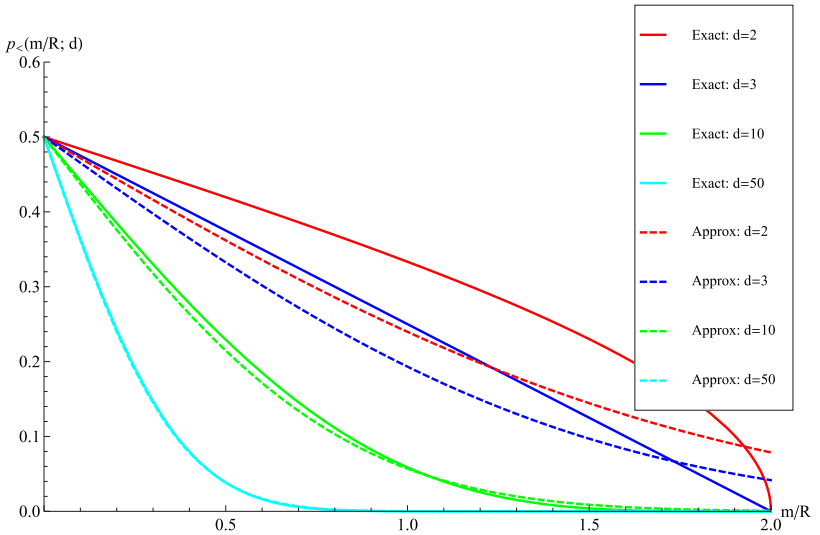

Fig. S7. Probability that a vector originating on the surface of a sphere has its end point within that sphere as a function of the vector size *m* (scaled to the radius of the sphere *R*). Several numbers of dimensions are shown. The plots labeled "Exact" show the exact result for $P < (m/R;d)$ from Eq. **S6**. The plots labeled "Approx" show the high-dimension approximation to this function originally used by Fisher, $p < (m/R;d) \approx \int_{\frac{m}{R}\sqrt{d}}^{\infty} e^{-\frac{t^2}{2}} dt$. The approximation is effective at high dimension but is inappropriate at low dimension.

Table S1. Probability of observing balanced polymorphisms during adaptive walks toward a fixed fitness optimum as a function of relative mutation sizes for various settings of population size N and SD σ_w of the Gaussian fitness function

N	σ_w	$\langle m \rangle$	$\langle m \rangle / r_0$	Adaptedness	P_{bal} (run)	P_{bal} (time)
10^3	1	1	22	0.90	0.91	0.45
	2	1	11	0.86	0.86	0.38
	5	1	4.5	0.61	0.70	0.22
	10	1	2.2	0.26	0.49	0.11
	20	1	1.1	0.06	0.34	0.04
10^4	1	1	71	0.98	0.96	0.50
	2	1	35	0.97	0.95	0.48
	5	1	14	0.92	0.89	0.39
	10	1	7.1	0.78	0.79	0.31
	20	1	3.5	0.50	0.63	0.17
	50	1	1.4	0.10	0.35	0.04
	100	1	0.71	0.00	0.30	0.02
10^5	1	1	224	1.00	0.98	0.52
	2	1	112	0.99	0.97	0.51
	5	1	45	0.99	0.95	0.47
	10	1	22	0.96	0.91	0.45
	20	1	11	0.88	0.86	0.38
	50	1	4.5	0.61	0.69	0.23
	100	1	2.2	0.25	0.48	0.11
	200	1	1.1	0.06	0.36	0.04
	400	1	0.56	0.00	0.32	0.02
10^4	10	0.5	3.5	0.72	0.65	0.17
	10	0.2	1.4	0.43	0.15	0.01
	10	0.1	0.71	0.16	0.04	0.00
	10	0.05	0.35	0.05	0.02	0.00

"Adaptedness" measures the average improvement in mean population fitness achieved over a walk relative to the maximally possible improvement: $(\langle w_{end} \rangle - \langle w_{start} \rangle)/(1 - \langle w_{start} \rangle)$. P_{bal} (run) is the probability of at least one balanced polymorphism arising over the course of the walk. P_{bal} (time) is the average time during which balanced polymorphisms are present over the walk. In the last four rows, N and σ_w were kept constant and the average mutation size $\langle m \rangle$ was varied instead. Statistics were obtained by averaging over 10^3 walks for each parameter setting. In accordance with our theoretically predicted limit, consequential balanced polymorphisms are common until the ratio $\langle m \rangle / r_0$ becomes on the order of 1 or less.

Table S2. Probability of observing balanced polymorphisms in adaptive walks toward a moving fitness optimum under different speeds of environmental change

σ_{env}	Runs extinct, %*	Time polymorphic, %†	Polymorphisms balanced, %‡	Substitutions balanced, %§
1	100	4	1	—
10^{-1}	25	38	44	68
10^{-2}	0	31	74	67
10^{-3}	0	29	85	67
10^{-4}	0	23	93	61
10^{-5}	0	5	58	—

For each speed σ_{env} of the optimum, 10^3 simulation runs of 10^7 generations each were simulated (*Materials and Methods*). Under the very fast-moving optimum ($\sigma_{env} = 1$), populations typically became extinct quickly and only a few polymorphisms were observed in the short time window before extinction. Those polymorphisms were mostly unbalanced. However, once the optimum moved slower, such that the population could effectively follow it, polymorphisms became common; typically, more than 50% of those polymorphisms were balanced. Under a very slowly moving optimum ($\sigma_{env} = 10^{-5}$), populations were well adapted most of the time, and thus again less frequently polymorphic. The fraction of balanced polymorphisms among all polymorphisms, however, remained substantial in this scenario. In all scenarios, a substantial fraction (60–70%) of the adaptive mutations that eventually became fixed in the population did go through an intermediate balanced state (these data have not been collected for the extremely fast-moving, $\sigma_{env} = 1$, and extremely slow-moving, $\sigma_{env} = 10^{-5}$, optima).

*Percentage of runs in which the population could not successfully follow the fitness optimum (extinction defined by the mean population fitness approaching zero).

†Percentage of time during which a polymorphism (frequency $0.05 < x < 0.95$) was present in the population averaged over runs (only the time before extinction was considered).

‡Percentage of polymorphisms that were balanced.

§Percentage of all observed substitutions that had ever been part of a balanced polymorphism.